Inorg. Chem. **1997,** *36,* 994−1003

Reactivity of Cubane-Type $[(OC)_3MFe_3S_4(SR)_3]^{3-}$ Clusters (M = Mo, W): Interconversion with Cuboidal $[Fe_3S_4]^0$ Clusters and Electron Transfer

James W. Raebiger, Charles A. Crawford, Jian Zhou, and R. H. Holm*

Department of Chemistry and Chemical Biology, Harvard University, Cambridge, Massachusetts 02138

Received September 11, 1996[⊗]

The title clusters, several examples of which have been reported earlier, have been prepared by two different methods and subjected to structural and reactivity studies. The compounds $(Et_4N)_3[(OC)_3MFe_3S_4(Smes)_3]\cdot MeCN$ (M = Mo/W) are isomorphous and crystallize in monoclinic space group $P2_1/n$ with $a = 13.412(1)/13.297(1)$ Å, $b = 19.0380(1)/18.9376(3)$ Å, $c = 26.4210(1)/26.2949(1)$ Å, $\beta = 97.87(1)/97.549(1)°$, and $Z = 4$. The clusters contain long M−S (2.62/2.59 Å) and M−Fe (3.22/3.19 Å) bonds, consistent with the reported structure of $[(OC)_3MoFe_3S_4(SEt)_3]^{3-}$ (**3**). Reaction of $[(OC)_3MoFe_3S_4(LS_3)]^{3-}$ (**7**) with CO in the presence of $NaPF_6$ affords cuboidal $[Fe_3S_4(LS_3)]^{3-}$ (**9**), also prepared in this laboratory by another route as a synthetic analogue of protein-bound $[Fe_3S_4]^0$ clusters. The clusters $[Fe_3S_4(SR)_3]^{3-}$ (R = mes, Et), of limited stability, were generated by the same reaction. Treatment of **9** with $[M(CO)_3(MeCN)_3]$ affords **7** and its M = W analogue. The clusters $[(OC)_3MFe_3S_4(SR)_3]^{3-}$ form a four-member electron transfer series in which the 3− cluster can be once reduced (4−) and twice oxidized (2−, 1−) to afford clusters of the indicated charges. The correct assignment of redox couple to potential in the redox series of six clusters is presented, correcting an earlier misassignment of the redox series of **3**. Carbonyl stretching frequencies are shown to be sensitive to cluster oxidation state, showing that the M sites and Fe_3S_4 fragments are electronically coupled despite the long bond distances. (LS_3 = 1,3,5-tris((4,6-dimethyl-3-mercaptophenyl)thio)-2,4,6-tris(*p*-tolylthio)benzenate(3−); mes = mesityl.)

Introduction

There are currently three recognized biological iron−sulfur clusters with nuclearity 4 or less: rhomboidal $Fe_2(\mu_2\text{-}S)_2$, cuboidal $Fe_3(\mu_3\text{-}S)(\mu_2\text{-}S)_3$, and cubane-type $Fe_4(\mu_3\text{-}S)_4$. Since the initial detection of a trinuclear cluster[1] and the subsequent structure proof of the cuboidal stereochemistry by protein crystallography,[2−5] a synthetic analogue **1**, $[Fe_3S_4(SR)_3]^{z-}$, of the cuboidal cluster has been conspicuous by its absence. In contrast, analogues of the other native clusters were prepared either previously to (Fe_2S_2) or essentially coincident with (Fe_4S_4) their proof by crystallography.[6] Recently, this situation was redressed with the synthesis and structural and electronic elucidation of the clusters $[Fe_3Q_4(LS_3)]^{3-}$ (Q = S, Se).[7−9] These clusters were obtained by reaction 1, which abstracts Fe(II) from

$$[Fe_4Q_4(LS_3)(CF_3SO_3)]^{2-} + 2Meida^{2-} \rightarrow [Fe_3Q_4(LS_3)]^{3-} + [Fe(Meida)_2]^{2-} + CF_3SO_3^{\ -} \quad (1)$$

the $[Fe_4S_4]^{2+}$ core of the initial cluster. The iron sites of this cluster are differentiated in a 1:3 ratio by the trithiolate ligand LS_3,[10,11] which induces regiospecific reactivity at the unique site. This investigation provided key information in relation to two important aspects of protein-bound clusters. First, $[Fe_3S_4(LS_3)]^{3-}$ is stable in acetonitrile for at least 1 week under anaerobic ambient conditions,[8] demonstrating that protein structure itself is not obligatory for stabilization of the cuboidal cluster, at least in the $[Fe_3S_4]^0$ oxidation state. However, the semirigid cavitand ligand LS_3[10b] does have a stabilizing effect on the cluster. Second, the nonclassical electron distribution and magnetic coupling affording an $S = 2$ ground state, involving a localized Fe^{3+} site and a delocalized $Fe^{3+}Fe^{2+}$ pair in proteins,[12] is reproduced exactly in the synthetic cluster, proving a negligible effect of protein structure and environment on electronic structure. Thus, the synthetic analogue has conveyed information intrinsic to the $[Fe_3S_4]^0$ state.[8] Additionally, the three-member electron transfer series $[Fe_3S_4(LS_3)]^{+,0,-}$ was established in an aprotic medium.[8]

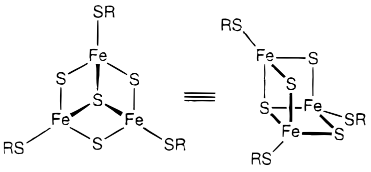

1

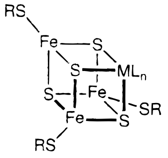

2

Other than electron transfer, the only established reactions of Fe_3S_4 clusters involve metal ion incorporation in the $[Fe_3S_4]^{0,-}$

[⊗] Abstract published in *Advance ACS Abstracts,* March 1, 1997.

(1) (a) Emptage, M. H.; Kent, T. A.; Huynh, B. H.; Rawlings, J.; Orme-Johnson, W. H.; Münck, E. *J. Biol. Chem.* **1980**, *255*, 1793. (b) Huynh, B. H.; Moura, J. J. G.; Moura, I.; Kent, T. A.; LeGall, J.; Xavier, A. V.; Münck, E. *J. Biol. Chem.* **1980**, *255*, 3242.

(2) Robbins, A. H.; Stout, C. D. *Proteins* **1989**, *5*, 289.

(3) (a) Kissinger, C. R.; Adman, E. T.; Sieker, L. C.; Jensen, L. H. *J. Am. Chem. Soc.* **1988**, *110*, 8721. (b) Kissinger, C. R.; Sieker, L. C.; Adman, E. T.; Jensen, L. H. *J. Mol. Biol.* **1991**, *219*, 693.

(4) (a) Stout, C. D. *J. Mol. Biol.* **1989**, *205*, 545. (b) Soman, J.; Iismaa, S.; Stout, C. D. *J. Biol. Chem.* **1991**, *266*, 21558. (c) Stout, C. D. *J. Biol. Chem.* **1993**, *268*, 25920.

(5) Merritt, E. A.; Stout, G. H.; Turley, S.; Sieker, L. C.; Jensen, L. H.; Orme-Johnson, W. H. *Acta Crystallogr.* **1993**, *D49*, 272.

(6) Berg, J. M.; Holm, R. H. In *Iron-Sulfur Proteins*; Spiro, T. G., Ed.; Wiley: New York, 1982; Chapter 1.

(7) Zhou, J.; Holm, R. H. *J. Am. Chem. Soc.* **1995**, *117*, 11353.

(8) Zhou, J.; Hu, Z.; Münck, E.; Holm, R. H. *J. Am. Chem. Soc.* **1996**, *118*, 1966.

(9) Abbreviations: LS_3, 1,3,5-tris((4,6-dimethyl-3-mercaptophenyl)thio)-2,4,6-tris(*p*-tolylthio)benzenate(3−); Meida, *N*-methylimidodiacetate-(2−); mes, mesityl; ttcn, 1,4,7-trithiacyclononane.

(10) (a) Stack, T. D. P.; Holm, R. H. *J. Am. Chem. Soc.* **1988**, *110*, 2484. (b) Stack, T. D. P.; Weigel, J. A.; Holm, R. H. *Inorg. Chem.* **1990**, *29*, 3745.

(11) Holm, R. H.; Ciurli, S.; Weigel, J. A. *Prog. Inorg. Chem.* **1990**, *29*, 1.

(12) Papaefthymiou, V.; Girerd, J.-J.; Moura, I.; Moura, J. J. G.; Münck, E. *J. Am. Chem. Soc.* **1987**, *109*, 4703.

S0020-1669(96)01122-6 CCC: $14.00

states to afford the heterometal MFe_3S_4 cubane clusters **2**. These reactions are known for both protein-bound[13,14] and synthetic clusters.[7,17] The latter can be prepared by other methods, including reductive rearrangement of "linear" $[Fe_3S_4(SR)_4]^{3-}$ precursor clusters[15,16] (vide infra). The insertion of closed-shell ions such as Zn(II),[14a,c,d,h] Cu(I),[14f] and Tl(I)[14g] results in small perturbations of the electronic structures of the protein-bound clusters, as reflected in EPR, Mössbauer, and MCD spectra and in significant changes in redox potentials.[14a,d,f,h] Paramagnetic heterometal ions such as Co(II) and Ni(II) lead to much larger electronic changes[14c,h] owing to the coupling of M and Fe_3S_4 spins. No X-ray structures are available for proteins with potential MFe_3S_4 clusters. The cubane formulation of MFe_3S_4 clusters is highly reasonable and is supported by a near-congruency of electronic properties between synthetic $CoFe_3S_4$ and $NiFe_3S_4$ clusters of known structures and those of proteins incubated with Co(II) and Ni(II).[15] By inference, other heterometal species with perturbed Fe_3S_4 protein centers are expected to have this structure.

Although no MFe_3S_4 cluster has been proven to exist in the *native* state, the pervasive occurrence of Fe_3S_4 clusters in a wide variety of proteins and enzymes[13,18] leads to the possibility of heterometal ion incorporation when the cluster is reduced to the $[Fe_3S_4]^0$ or lower oxidation state. Putative protein-bound MFe_3S_4 clusters might modulate redox potentials, influence metal ion concentrations by complexation, and contribute to protein structure by binding of a side chain group. Given the evolving biological considerations of Fe_3S_4 clusters, we are continuing our investigation of synthetic clusters of this type, in order to disclose their fundamental structural and reactivity properties. Among such clusters, we note that the synthesis of $[Fe_3S_4(LS_3)]^{3-}$ was preceded by preparation of $[Fe_4S_4(LS_3)(RNC)_3]^{-}$ [19] and $[(OC)_3MoFe_3S_4(SR)_3]^{3-}$,[16] which in formulation **2** contain the fragment $[Fe_3S_4]^0$ and the units $ML_n = Fe^{II}(CNR)_3$ and $Mo^0(CO)_3$, respectively, whose metal atoms are diamagnetic. These species have an $S = 2$ ground state and are properly described as mildly perturbed versions of the $[Fe_3S_4]^0$ state. In this work, we demonstrate that $[(OC)_3MoFe_3S_4(LS_3)]^{3-}$ and $[Fe_3S_4(LS)_3]^{3-}$ can be interconverted.

Any attempts to understand the effect of an ML_n group on the redox potential of its MFe_3S_4 cluster vs that of an unperturbed Fe_3S_4 cluster are best made at equality of charge in the redox couples. If the original assignment of potentials to the 2−/3− and 3−/4− redox couples of $[(OC)_3MoFe_3S_4(SR)_3]^{3-}$ [16] is accepted, comparison with the corresponding couples of $[Fe_3S_4(LS_3)]^{3-}$ leads to apparent stabilization of the $[Fe_3S_4]^+$ and $[Fe_3S_4]^0$ states by *ca.* 0.5−0.6 and 0.6−0.8 V (vide infra), respectively. These effects would arise by the introduction of the neutral $Mo(CO)_3$ group into the $[Fe_3S_4]^0$ core. Such differences in potential were considered by us to be unexpectedly large[8] and, if correct, must be understood in relation to the general question of the effect of variant heterometal groups on the relative redox potentials of both synthetic and protein-bound MFe_3S_4 clusters. We have investigated this seemingly large discrepancy in redox potentials and report our results and conclusions herein.

Experimental Section[9]

Preparation of Compounds. All manipulations were performed under a pure dinitrogen atmosphere using standard glovebox and Schlenk techniques. Solvents were dried and degassed prior to use. The compounds $(Et_4N)_3[Fe_3S_4(LS_3)]$,[8] $[M(CO)_3(MeCN)_3]$ (M = Mo, W),[20] $[M(CO)_3(ttcn)]$ (M = Mo,[21] W[22]), 2,4,6-trimethylbenzenethiol,[23] and $L(SH)_3$[10] were prepared by literature procedures. The products of the following preparations were substantially or highly pure by an ^{1}H NMR criterion; spectra were measured at 297 K.

(a) $(Et_4N)_3[(OC)_3MFe_3S_4(SEt)_3]$ (M = Mo, W). The M = Mo compound was prepared by a literature procedure.[16] ^{1}H NMR (CD_3CN): δ 66.3 (CH_2), 6.15 (CH_3). IR (acetonitrile): ν_{CO} 1871, 1761 cm^{-1}. The M = W compound was prepared by an analogous method using $[W(CO)_3(MeCN)_3]$. ^{1}H NMR (CD_3CN): δ 66.1 (CH_2), 5.79 (CH_3). IR (acetonitrile): ν_{CO} 1860, 1756 cm^{-1}.

(b) $(Et_4N)_3[(OC)_3MoFe_3S_4(Smes)_3]$. To a stirred solution of 200 mg (0.190 mmol) of $(Et_4N)_3[(OC)_3MoFe_3S_4(SEt)_3]$ in 50 mL of acetonitrile was added a solution of 90 mg (0.570 mmol) of 2,4,6-trimethylbenzenethiol in 5 mL of acetonitrile. The reaction mixture was stirred for 2 h, and the solvent was removed in vacuo. The resulting brown solid was washed with 10 mL of THF and 3 × 5 mL of acetone. The solid was dissolved in 50 mL of acetonitrile, and the solution was filtered. The filtrate was reduced to dryness in vacuo to afford 217 mg (86%) of product as a brown solid. Absorption spectral data (acetonitrile), λ_{max}, nm (ϵ_M): 249 (sh, 35 700), 337 (20 400), 390 (19 100), ~570 (sh, 2500). IR (acetonitrile): ν_{CO} 1872, 1766 cm^{-1}. ^{1}H NMR (CD_3CN): δ 14.75 (*m*-H), 12.28 (*p*-Me), 10.67 (*o*-Me). This compound was additionally identified by an X-ray structure determination.

(c) $(Et_4N)_3[(OC)_3WFe_3S_4(Smes)_3]$. To a stirred solution of 300 mg (0.264 mmol) of $(Et_4N)_3[(OC)_3WFe_3S_4(SEt)_3]$ in 50 mL of acetonitrile was added a solution of 132 mg (0.870 mmol) of 2,4,6-trimethylbenzenethiol in 5 mL of acetonitrile. The reaction mixture was stirred for 2 h, and the solvent was removed in vacuo. The resulting brown solid was washed with 10 mL of THF and 3 × 5 mL of acetone. The solid was dissolved in 20 mL of acetonitrile, and the solution was filtered. The filtrate was layered with ether, causing over 3 d the separation of product as 325 mg (87%) of brown crystals. Absorption spectral data (acetonitrile), λ_{max}, nm (ϵ_M): 251 (sh, 41 700), 339 (24 500), 394 (23 300), 570 (sh, 2500). IR (acetonitrile): ν_{CO} 1861, 1763 cm^{-1}. ^{1}H NMR (CD_3CN): δ 14.75 (*m*-H), 12.12 (*p*-Me), 10.59 (*o*-Me). This compound was additionally identified by an X-ray structure determination.

(d) $(Et_4N)_3[(OC)_3MoFe_3S_4(LS_3)]$. Method A. To a stirred solution of 110 mg (0.0672 mmol) of $(Et_4N)_3[Fe_3S_4(LS_3)]$ in 30 mL of acetonitrile was added a solution of 24.9 mg (0.101 mmol) of $[Mo(CO)_3(MeCN)_3]$ in 5 mL of acetonitrile. The reaction mixture was stirred for 30 min, and 50 mL of ether was added, resulting in the separation of product as 122 mg (90%) of purple-black solid. Absorp-

---

(13) Holm, R. H. *Adv. Inorg. Chem.* **1992**, *38*, 1.

(14) (a) Butt, J. N.; Armstrong, F. A.; Breton, J.; George, S. J.; Thomson, A. J.; Hatchikian, E. C. *J. Am. Chem. Soc.* **1991**, *113*, 6663. (b) Thomson, A. J.; Breton, J.; Butt, J. N.; Hatchikian, E. C.; Armstrong, F. A. *J. Inorg. Biochem.* **1992**, *47*, 197. (c) Srivastava, K. K. P.; Surerus, K. K.; Conover, R. C.; Johnson, M. K.; Park, J.-B.; Adams, M. W. W.; Münck, E. *Inorg. Chem.* **1993**, *32*, 927. (d) Moreno, C.; Macedo, A. J.; Moura, I.; LeGall, J.; Moura, J. J. G. *J. Inorg. Biochem.* **1994**, *53*, 219. (e) Faridoon, K. Y.; Zhuang, H.-Y.; Sykes, A. G. *Inorg. Chem.* **1994**, *33*, 2209. (f) Butt, J. N.; Niles, J.; Armstrong, F. A.; Breton, J.; Thomson, A. J. *Nat. Struct. Biol.* **1994**, *1*, 427. (g) Fu, W.; Telser, J.; Hoffman, B. M.; Smith, E. T.; Adams, M. W. W.; Finnegan, M. G.; Conover, R. C.; Johnson, M. K. *J. Am. Chem. Soc.* **1994**, *116*, 5722. (h) Finnegan, M. G.; Conover, R. G.; Park, J.-B.; Zhou, Z. H.; Adams, M. W. W.; Johnson, M. K. *Inorg. Chem.* **1995**, *34*, 5358.

(15) (a) Ciurli, S.; Ross, P. K.; Scott, M. J.; Yu, S.-B.; Holm, R. H. *J. Am. Chem. Soc.* **1992**, *114*, 5415. (b) Zhou, J.; Scott, M. J.; Hu, Z.; Peng, G.; Münck, E.; Holm, R. H. *J. Am. Chem. Soc.* **1992**, *114*, 10843.

(16) (a) Coucouvanis, D.; Al-Ahmad, S.; Salifoglou, A.; Dunham, W. R.; Sands, R. H. *Angew. Chem., Int. Ed. Engl.* **1988**, *27*, 1353. (b) Coucouvanis, D.; Al-Ahmad, S.; Salifoglou, A.; Papaefthymiou, V.; Kostikas, A.; Simopoulos, A. *J. Am. Chem. Soc.* **1992**, *114*, 2472.

(17) Zhou, J.; Raebiger, J. W.; Crawford, C. A.; Holm, R. H., submitted for publication.

(18) Cammack, R. *Adv. Inorg. Chem.* **1992**, *38*, 281. For example, note the recent crystallographic proof of an Fe_3S_4 cluster in a [NiFe] hydrogenase: Volbeda, A.; Charon, M. H.; Piras, C.; Hatchikian, E. C.; Frey, M.; Fontecilla-Camps, J. C. *Nature* **1995**, *373*, 580.

(19) Weigel, J. A.; Srivastava, K. K. P.; Day, E. P.; Münck, E.; Holm, R. H. *J. Am. Chem. Soc.* **1990**, *112*, 8015.

(20) Tate, D. P.; Knipple, W. R.; Augl, J. M. *Inorg. Chem.* **1962**, *1*, 433.

(21) Ashby, M. T.; Lichtenberger, D. L. *Inorg. Chem.* **1985**, *24*, 636.

(22) Kim, H.-J.; Do, Y.; Lee, H. W.; Jeong, J. H.; Sohn, Y. S. *Bull. Korean Chem. Soc.* **1991**, *12*, 257.

(23) Chisholm, M.; Corning, J. F.; Huffman, J. C. *Inorg. Chem.* **1984**, *23*, 754.

tion spectral data (acetonitrile), λ_{max}, nm (ϵ_M): 259 (sh, 92 000), 305 (sh, 47 500), 508 (12 200) nm. IR (acetonitrile): ν_{CO} 1875, 1768 cm^{-1}. ^{1}H NMR (Me$_2$SO): δ 15.37 (5-H), 13.00 (6-Me), 8.96 (4-Me), 7.40 (2′-H), 6.41 (3′-H), 2.32 (4′-Me).

Method B. A mixture of 200 mg (0.190 mmol) of $(Et_4N)_3[(OC)_3MoFe_3S_4(SEt)_3]$, 200 mg (0.211 mmol) of L(SH)$_3$, and 240 mg (0.570 mmol) of $(Bu_4N)(BF_4)$ in 50 mL of acetonitrile was stirred for 2 h and filtered. The filtrate was reduced to dryness in vacuo. The resulting purple-black solid was washed with 10 mL of THF and 3 × 5 mL of acetonitrile. It was then dissolved in 50 mL of acetonitrile, and the solution was filtered. The solvent was removed in vacuo, leaving 180 mg (50%) of product as a purplish-black solid, identical in all respects to the product of method A.

(e) $(Et_4N)_3[(OC)_3WFe_3S_4(LS_3)]$. To a stirred solution of 300 mg (0.184 mmol) of $(Et_4N)_3[Fe_3S_4(LS_3)]$ in 50 mL of acetonitrile was added a solution of 115 mg (0.294 mmol) of $[W(CO)_3(MeCN)_3]$ in 10 mL of acetonitrile. The reaction mixture was stirred for 30 min, and 50 mL of ether was added, resulting in the separation of product as 210 mg (60%) of purple-black solid. Absorption spectral data (acetonitrile): λ_{max}, nm (ϵ_M): 260 (sh, 95 700), 306 (sh, 49 200), 519 (13 100). IR (acetonitrile): ν_{CO} 1864, 1767 cm^{-1}. ^{1}H NMR (Me$_2$SO): δ 15.24 (5-H), 13.13 (6-Me), 8.77 (4-Me), 7.46 (2′-H), 6.50 (3′-H), 2.37 (4′-Me).

The following three clusters were generated in solution by the indicated reactions; isolation and full characterization of $[Fe_3S_4(LS_3)]^{3-}$ prepared by a different method in the absence of sodium salts are described elsewhere.[8]

(f) $[NaFe_3S_4(LS_3)]^{2-}$. A solution of 1.63 mg (9.71 μmol) of NaPF$_6$ in 0.1 mL of acetonitrile was added to a solution of 3.55 mg (1.96 μmol) of $(Et_4N)_3[(OC)_3MoFe_3S_4(LS_3)]$ in 0.5 mL of acetonitrile. Carbon monoxide was slowly bubbled through the solution for 2 min. When the reaction was conducted in CD$_3$CN, the ^{1}H NMR spectrum was recorded: δ 13.58 (5-H), 11.49 (6-Me), 9.07 (4-Me), 7.91 (2′-H), 6.76 (3′-H), 2.44 (4′-Me). No other cluster resonances were observed.

(g) $[NaFe_3S_4(Smes)_3]^{2-}$. A solution of 27.8 mg (166 μmol) of NaPF$_6$ in 0.1 mL of acetonitrile was added to a solution of 22.0 mg (16.6 μmol) of $(Et_4N)_3[(OC)_3MoFe_3S_4(Smes)_3]^{3-}$ in 0.5 mL of acetonitrile. Carbon monoxide was slowly bubbled through the solution for 2 min. When the reaction was conducted in CD$_3$CN, the ^{1}H NMR spectrum was recorded: δ 14.06 (*m*-H), 9.30 (*p*-Me), 8.05 (*o*-Me). No other cluster resonances were observed.

(h) $[NaFe_3S_4(SEt)_3]^{2-}$. A solution of 3.00 mg (2.86 μmol) of $(Et_4N)_3[(OC)_3MoFe_3S_4(SEt)_3]$ in 0.3 mL of CD$_3$CN was treated with 4.80 mg (28.6 μmol) of NaPF$_6$ in 0.2 mL of CD$_3$CN. The solution was kept under a CO stream for 10 min and the reaction monitored by ^{1}H NMR. At this point, 25% of the cluster products was the cuboidal species: δ 57.9 (CH$_2$), 5.09 (CH$_3$). The remaining 75% was $[Fe_4S_4(SEt)_4]^{2-}$: δ 12.7 (CH$_2$), 3.00 (CH$_3$). After 1 h, only the latter cluster was detectable.

X-ray Structure Determinations. Suitable crystals of $(Et_4N)_3[(OC)_3MFe_3S_4(Smes)_3]$ (M = Mo, W) were grown by vapor diffusion of ether into acetonitrile solutions. These were coated with grease, attached to glass fibers, and transferred to a Nicolet P3F (M = Mo) or Siemens SMART (M = W) diffractometer. Lattice parameters were obtained from least-squares analysis of 26 ($20 \le 2\theta \le 30°$, M = Mo) or 100 ($10 \le 2\theta \le 20°$, M = W) machine-centered reflections. Neither compound showed any significant decay over the course of data collection. The raw intensity data were converted to structure factor amplitudes and their esd's by correction for scan speed, background, and Lorentz and polarization effects using the program XDISK (M = Mo) or SAINT (M = W) of SHELXTL PLUS. Empirical absorption corrections were applied by using the program XEMP. The two compounds are isomorphous. Crystallographic data are summarized in Table 1. The space group was identified by systematic absences. The structure was solved by direct methods and refined by standard least-squares and Fourier techniques. All non-hydrogen atoms in the M = W structure and all but one cation and the acetonitrile solvate molecule in the M = Mo structure were refined anisotropically. Hydrogen atoms were assigned idealized locations and given a uniform value for B_{iso} of 0.8 Å^2. The asymmetric units consist of three cations, one anion, and one acetonitrile solvate molecule. In the last cycles of refinement, all parameters shifted by less than 1% of their esd's, and the final difference Fourier maps showed no significant electron density.[24]

Table 1. Data Collection and Crystal Parameters[a] for $(Et_4N)_3[(OC)_3MFe_3S_4(Smes)_3]\cdot MeCN$ (M = Mo, W)

	M = Mo	M = W
empirical formula	$C_{56}H_{93}Fe_3MoN_4O_3S_7$	$C_{56}H_{93}Fe_3N_4O_3S_7W$
fw	1358.25	1446.16
crystal system	monoclinic	monoclinic
space group	$P2_1/n$	$P2_1/n$
λ, Å	0.71073	0.71073
a, Å	13.412(1)	13.2971(1)
b, Å	19.0380(3)	18.9376(3)
c, Å	26.4210(1)	26.2949(1)
β, deg	97.87(1)	97.549(1)
V, Å^3	6682.7(1)	6564.1(1)
Z	4	4
ρ_{calc}, g/cm^3	1.350	1.463
μ, mm^{-1}	2.661	1.082
T, °C	−50	−60
crystal size, mm^3	0.5 × 0.5 × 0.2	0.3 × 0.3 × 0.15
2θ range, deg	3.0−47.0	2.7−47
R,[a] w$R2$[b]	5.88, 12.48	5.40, 13.62

[a] $R = \sum||F_o| - |F_c||/\sum|F_o|$. [b] $wR2 = \{\sum[w(F_o^2 - F_c^2)^2]/\sum[w(F_o^2)^2]\}^{1/2}$.

Other Physical Measurements. ^{1}H NMR spectra were recorded on Bruker AM500 and AM400 spectrometers. Mössbauer spectroscopic measurements were made as previously described;[25] isomer shifts are relative to iron metal at room temperature. Electrochemical measurements were performed with a PAR Model 263 potentiostat/galvanostat using a Pt working electrode. The supporting electrolyte was $(Bu_4N)(PF_6)$, 0.1 M for cyclic voltammetry and 0.5 M for controlled-potential coulometry in acetonitrile solutions. Potentials are referenced to the SCE. Certain redox reactions were followed by IR spectroscopy using an optically transparent thin-layer electrode (OTTLE) cell equipped with a Au mesh working electrode, a Pt auxiliary electrode, and a Ag wire pseudoreference electrode. The cell design followed that of Krejčik *et al.*[26]

Results and Discussion

The following clusters and complexes **3**−**14** are of principal interest in this investigation. Species **3**, **9**, **13**, and **14** have been described in some detail previously; clusters **5**−**8** and **10**−**12** originate with this work. Schematic structures and the methods of preparation of clusters **3**−**11** are given in Figure 1. We are especially concerned with the synthesis and reactivity of the heterometal tricarbonyl clusters **3**−**8**.

$[(OC)_3MFe_3S_4(SEt)_3]^{3-}$	M = Mo (**3**[15]), W (**4**[15])
$[(OC)_3MFe_3S_4(Smes)_3]^{3-}$	M = Mo (**5**), W (**6**)
$[(OC)_3MFe_3S_4(LS_3)]^{3-}$	M = Mo (**7**), W (**8**)
$[Fe_3S_4(LS_3)]^{3-}$	**9**[7,8]
$[NaFe_3S_4(LS_3)]^{2-}$	**10**
$[NaFe_3S_4(Smes)_3]^{2-}$	**11**
$[NaFe_3S_4(SEt)_3]^{2-}$	**12**
$[M(CO)_3(ttcn)]$	M = Mo (**13**[21]), W (**14**[22])

MFe$_3$S$_4$ Cluster Synthesis and Structure (M = Mo, W). Molybdenum cluster **3** was first prepared by Coucouvanis *et al.*[16] using the reductive rearrangement reaction shown in Figure 1. Here the reductant required to achieve the Fe$^{2.67+}$ oxidation state of the product (assuming Mo(0); vide infra) is most likely an ethanethiolate ligand of the initial trinuclear iron cluster. We have confirmed this preparation and its extension to the tungsten cluster **4**, which has been mentioned but without characterization data.[16b] Here we have provided ^{1}H NMR and IR data for **4**. Clusters of the type $[(OC)_3MoFe_3S_4L_3]^{3-}$ (L = RS$^-$,

---

(24) See paragraph at end of paper regarding Supporting Information.

(25) MacDonnell, F. M.; Ruhlandt-Senge, K.; Ellison, J. J.; Holm, R. H.; Power, P. P. *Inorg. Chem.* **1995**, *34*, 1815.

(26) Krejčik, M.; Daněk, M.; Hartl, F. *J. Electroanal. Chem. Interfacial Electrochem.* **1991**, *317*, 179.

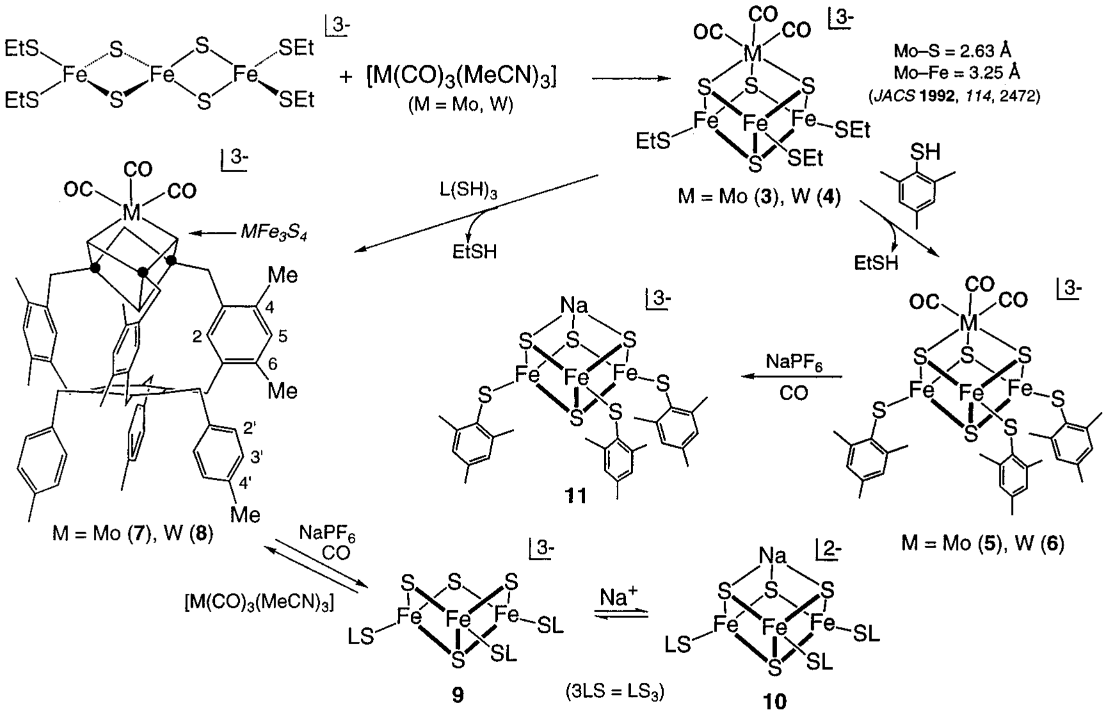

Figure 1. Synthetic routes to complexed (**3**–**6, 10, 11**) and free (**9**) $[Fe_3S_4]^0$ clusters. Cluster **11** is assumed to be in equilibrium with the free cluster $[Fe_3S_4(Smes)_3]^{3-}$ (not shown). The structures of the Na$^+$-perturbed clusters **10** and **11** are postulated, not proven. Note the numbering system for the LS$_3$ ligand system used in ^{1}H NMR signal assignments of clusters **7**–**10**.

Table 2. Mössbauer Parameters (mm/s) and Magnetic Moments

	site 1		site 2			
cluster	δ^a	ΔE_Q	δ^a	ΔE_Q	μ_{eff},^{b} μ_B	ref
$(Et_4N)_3[(OC)_3MoFe_3S_4(SEt)_3]$ (**3**)	0.48^c	0.95	0.35	0.62		16b
$(Et_4N)_3[(OC)_3MoFe_3S_4(Smes)_3]$ (**5**)	0.49^c	1.32	0.34	0.51	5.09	*d*
$(Et_4N)_3[(OC)_3MoFe_3S_4(LS)_3]$ (**7**)	0.49^c	1.32	0.37	0.65	5.35	*d*
$(Et_4N)_3[Fe_3S_4(LS_3)]$ (**9**)	0.49^{c,e}	1.2, 1.5	0.35	0.5		8
$[NaFe_3S_4(LS_3)]^{2-}$ (**10**)	0.44^f	1.06	0.41	0.69	5.06	*d*
$[NaFe_3S_4(Smes)_3]^{2-}$ (**11**)					5.18	*d*

[a] Relative to Fe metal at room temperature. [b] Measured in acetonitrile solution (297 K) by a standard NMR method. [c] 4.2 K. [d] This work. [e] Three-site fit. [f] DMF/acetonitrile (1:1 v/v), 77 K.

RO$^-$) on standing in acetonitrile solutions overnight are reported to generate ^{1}H NMR signals ascribable to $[Fe_6S_9(SEt)_2]^{4-}$, $[Fe_4S_4(SEt)_4]^{2-}$, and other $[Fe_4S_4L_4]^{2-}$ species.[16] We have not observed this behavior, finding instead that anaerobic solutions of **3** and **4** are stable for days at ambient temperature. Clusters **5**–**7** were prepared by the ligand substitution reaction (2) (Figure 1) and obtained in yields of 86–87% (**5**, **6**) and 50% (**7**). The metal atom capture reaction (3) (M = Mo, W) *in situ* in acetonitrile solution is quantitative by ^{1}H NMR; workup affords the product clusters **7** (90%) and **8** (60%) in the indicated yields.

$$[(OC)_3MFe_3S_4(SEt)_3]^{3-} + 3RSH \rightarrow [(OC)_3MFe_3S_4(SR)_3]^{3-} + 3EtSH \quad (2)$$

$$[Fe_3S_4(LS_3)]^{3-} + [M(CO)_3(MeCN)_3] \rightarrow [(OC)_3MFe_3S_4(LS_3)]^{3-} + 3MeCN \quad (3)$$

Because clusters **5**–**8** contain the $[Fe_3S_4]^0$ fragment, for which S = 2 has been proven in the closely related species **3**,[16] the isotropically shifted proton resonances of the 2,4,6-trimethylbenzenethiolate and the coordinating arms of the LS$_3$ (substituents 4–6, Figure 1) ligands should fall in or near the 8–16 ppm range for cuboidal **9** (S = 2) in acetonitrile.[8] The spectra in Figure 2 demonstrate that this is the case. The pattern of isotropic shifts, ring proton and methyl groups negative (downfield), is consistent with dominant or exclusive contact interactions,[15b] in which case isotropic shifts are directly proportional to magnetic susceptibility.[27] The magnetic moments of **5** and **7** in acetonitrile, contained in Table 2, are consistent with a quintet state. The Mössbauer spectra of polycrystalline $(Et_4N)_3$[**5**] and $(Et_4N)_3$[**7**], shown in Figure 3, consist of two overlapping quadrupole doublets in a 1:2 intensity ratio. The Mössbauer parameters of these clusters (Table 2) are consistent with the prevailing description of the electronic structure of the S = 2 state.[12] Here a localized Fe^{3+} ion ($S = {}^5/_2$, site 1) is antiferromagnetically coupled to the double-exchange coupled, delocalized Fe^{3+}Fe^{2+} pair ($S = {}^9/_2$, site 2), affording the system spin S = 2. The isomer shifts are in accord with the indicated oxidation states. These clusters also exhibit the A$_1$ and E carbonyl stretching vibrations consistent with a trigonal M(CO)$_3$ group.

In further characterization, the structures of $(Et_4N)_3$[**5**]·MeCN and $(Et_4N)_3$[**6**]·MeCN were determined by X-ray analysis. The two compounds are isomorphous and virtually isometric. Structural details closely follow those of **3**;[16] consequently, no detailed discussion of the entire structures is necessary. Metric data are summarized in Table 3; the structure of tungsten cluster **6** is shown in Figure 4. Excluding the mesityl groups, the clusters have idealized C_{3v} symmetry, with trigonally distorted octahedral coordination at the molybdenum/tungsten atoms and distorted tetrahedral coordination at the iron sites. Except for the M–Fe and M–S distances, dimensions of the MFe$_3$S$_4$ core units are unexceptional compared to those of typical single cubanes, such as

---

(27) $(\Delta H/H_0)_{iso} = (\Delta H/H_0)_{dia} - (\Delta H/H_0)_{obs}$: Bertini, I.; Luchinat, C. *NMR of Paramagnetic Molecules in Biological Systems*; Benjamin/Cummings: Menlo Park, CA, 1986; Chapter 2.

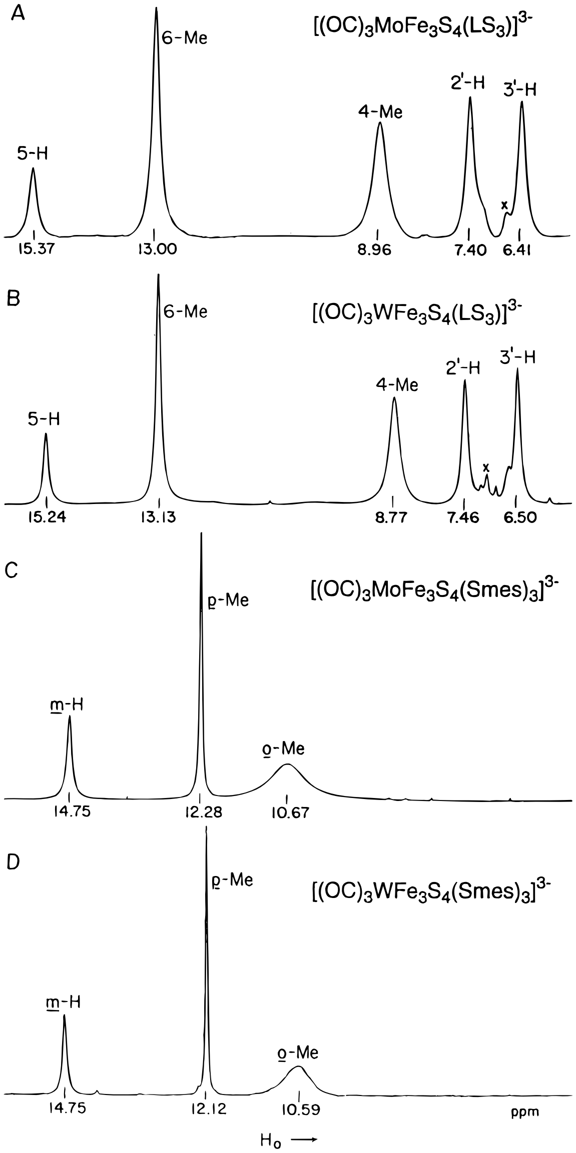

Figure 2. ^{1}H NMR spectra of $[(OC)_3MFe_3S_4(LS_3)]^{3-}$ [M = Mo (A), W (B)] in Me$_2$SO solutions and $[(OC)_3MFe_3S_4(Smes)_3]^{3-}$ [M = Mo (C), W (D)] in CD$_3$CN solutions at 297 K. Signal assignments are indicated; × = impurity. In spectra A and B, the 2-H resonances were not located and the 4′-Me resonances (not shown) occur at 2.3−2.4 ppm.

$[(NC)(C_6Cl_4O_2)MoFe_3S_4(SEt)_3]^{3-}$ [28] and $[(Meida)MoFe_3S_4Cl_3]^{2-}$,[29] and the individual WFe$_3$S$_4$ clusters in the bridged double cubane $[W_2Fe_7S_8(SCH_2Ph)_{12}]^{4-}$.[30] In these clusters, where the heterometal is tightly integrated structurally and electronically into an $[MFe_3S_4]^{3+}$ core, the mean values of M−Fe and M−S distances are in the narrow ranges 2.73−2.74 and 2.35−2.38 Å, respectively. The corresponding distances in **5**/**6** are 0.45−0.49 and 0.21−0.27 Å *longer* and are entirely comparable to those in **3**. Thus, with three structures in hand, it is clear that **3** is not unique and that long M−Fe and M−S core bonds are intrinsic properties of clusters compounded from $[Fe_3S_4]^0$ and d^6 M(CO)$_3$ fragments. Evidently, the three additional electrons carried by the M(CO)$_3$ group into $[MFe_3S_4]^0$ core formation are antibonding with respect to M−Fe and M−S interactions. This situation, together with the neutrality of the group, affords long bonds which, as will be seen, potentiate the lability of the M(CO)$_3$ group.

MFe$_3$S$_4$ → Fe$_3$S$_4$ Cluster Conversion. The structural features of clusters **5** and **6** imply lability of the M(CO)$_3$ groups in the set **3**−**8**.

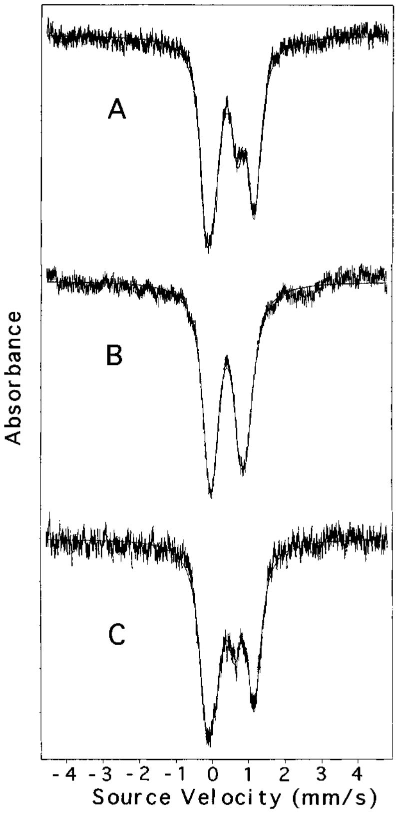

Figure 3. Zero-field Mössbauer spectra: polycrystalline $(Et_4N)_3[(OC)_3MoFe_3S_4(LS_3)]$ (A) at 4.2 K, $[NaFe_3S_4(Smes)_3]^{2-}$ (B) in DMF/acetonitrile (1:1 v/v) at 80 K, and polycrystalline $(Et_4N)_3[(OC)_3MoFe_3S_4(Smes)_3]$ (C) at 4.2 K.

Prior to the present work, it was reported that reaction of **3** with FeCl$_2$ in acetonitrile afforded the cubane clusters $[Fe_4S_4(SEt)_{4-n}Cl_n]^{2-}$.[16] We have examined the Mo(CO)$_3$ clusters **3**, **5**, and **7** as possible precursors to cuboidal $[Fe_3S_4]^0$. Certain results have been briefly described;[7] a fuller account is provided here. All reactions were carried out anaerobically in acetonitrile solutions and were monitored by ^{1}H NMR and IR spectroscopy.

Initial experiments were performed with cluster **7**, whose LS$_3$ ligand engenders stability to the cuboidal core.[8] Passage of CO through an acetonitrile solution of **7** at 1 atm for 2−3 h, with the intention of removing Mo(CO)$_3$ as $[Mo(CO)_{6-n}(MeCN)_n]$ (n = 0−3),[31] gave no indication of reaction. However, the addition of NaPF$_6$ to a solution of **7** (CO absent) led to a much different result. In solutions with $[\mathbf{7}]_0$ = 3.6 mM, the initial mole ratio of NaPF$_6$:**7** = 40:1 gave a 22% conversion of the initial cluster to cuboidal **10** after 1 h. As this ratio was increased, the extent of conversion increased, and with a ratio of (300−400):1 reached 75% at 1 h. Quantitative conversion was achieved by placing a solution of $[\mathbf{7}]_0$ = 3.6 mM and NaPF$_6$:**7** = 35:1 under a CO atmosphere (1 atm) for less than 1 h. The system is described by reaction 4 (n = 0−3) and is shown schematically in Figure 1. The product **10** is identified by chemical shifts which are close to those of

$$[(OC)_3MFe_3S_4(SR)_3]^{3-} + n\text{CO} + (3-n)\text{MeCN} + \text{Na}^+ \rightarrow [NaFe_3S_4(SR)_3]^{2-} + [Mo(CO)_{3-n}(MeCN)_{3-n}] \quad (4)$$

9 in acetonitrile in the absence of Na$^+$ (5-H, 15.48; 6-Me, 11.66; 4-Me, 8.51 ppm).[8] More practically, **10** can be fully generated in minutes when CO is passed through solutions with NaPF$_6$:**7** ≈ 10:1. The ^{1}H NMR spectrum of **10** formed under these conditions is provided in Figure 5; resonances of the coordinated portion of the LS$_3$ ligand occur at 9−14 ppm. The value $\mu_{\text{eff}} = 5.06\ \mu_B$ is indicative of an $S = 2$ state. No other cluster resonances are observed over a wide sweep range.

---

(28) Palermo, R. E.; Singh, R.; Bashkin, J. K.; Holm, R. H. *J. Am. Chem. Soc.* **1984**, *106*, 2600.

(29) Demadis, K. D.; Coucouvanis, D. *Inorg. Chem.* **1995**, *34*, 436.

(30) Wolff, T. E.; Berg, J. M.; Power, P. P.; Hodgson, K. O.; Holm, R. H. *Inorg. Chem.* **1980**, *19*, 430.

(31) Ross, B. L.; Grasselli, J. G.; Ritchey, W. M.; Kaesz, H. D. *Inorg. Chem.* **1963**, *2*, 1023. These complexes were characterized by IR spectroscopy.

Table 3. Selected Interatomic Distances (Å) and Angles (deg) for $[(OC)_3MFe_3S_4(Smes)_3]^{3-}$ (M = Mo, W)

Distances

	M = Mo	M = W		M = Mo	M = W
Fe1−S4	2.315(2)	2.299(2)	M−S1	2.612(2)	2.577(2)
Fe2−S4	2.321(2)	2.309(2)	M−S2	2.609(2)	2.574(2)
Fe3−S4	2.301(2)	2.282(2)	M−S3	2.641(2)	2.606(2)
mean of 3	2.312	2.297	mean of 3	2.621	2.586
Fe1−S1	2.269(3)	2.255(2)	M−C1	1.908(12)	1.921(10)
Fe1−S3	2.254(3)	2.252(2)	M−C2	1.942(10)	1.929(9)
Fe2−S2	2.277(2)	2.267(2)	M−C3	1.934(11)	1.936(11)
Fe2−S3	2.253(2)	2.249(2)	mean of 3	1.928	1.929
Fe3−S1	2.273(2)	2.260(2)			
Fe3−S2	2.263(2)	2.259(2)	S5−C4	1.767(8)	1.761(9)
mean of 6	2.265	2.257	S6−C13	1.805(9)	1.796(9)
			S7−C22	1.756(11)	1.768(10)
Fe1−S5	2.310(3)	2.300(3)			
Fe2−S6	2.314(3)	2.295(3)	C1−O1	1.193(11)	1.168(11)
Fe3−S7	2.299(3)	2.282(2)	C2−O2	1.162(10)	1.169(10)
			C3−O3	1.174(11)	1.168(12)
M−Fe1	3.283(1)	3.260(1)			
M−Fe2	3.266(1)	3.238(1)	Fe1−Fe2	2.689(2)	2.681(2)
M−Fe3	3.121(1)	3.084(1)	Fe1−Fe3	2.772(2)	2.758(2)
mean of 3	3.223	3.194	Fe2−Fe3	2.763(2)	2.755(2)
			mean of 3	2.741	2.731

Angles

	M = Mo	M = W		M = Mo	M = W
M−S1−Fe1	84.24(8)	84.58(7)	S1−M−S3	85.77(7)	86.11(7)
M−S1−Fe3	79.09(7)	78.93(7)	S1−M−S2	91.08(7)	91.95(7)
M−S2−Fe2	83.57(8)	83.70(7)	S2−M−S3	86.50(7)	87.02(6)
M−S2−Fe3	79.31(7)	79.02(7)			
M−S3−Fe1	83.85(8)	83.98(7)	Fe1−S1−Fe3	75.22(8)	75.29(7)
M−S3−Fe2	83.31(7)	83.33(7)	Fe1−S3−Fe2	73.24(7)	73.13(7)
mean of 6	82.23	82.26	Fe2−S2−Fe3	74.97(8)	74.98(7)
			mean of 3	74.48	74.47
S4−Fe1−S5	108.78(10)	108.78(9)			
S4−Fe2−S6	109.16(10)	109.27(10)	Fe1−S4−Fe2	70.90(7)	71.15(7)
S4−Fe3−S7	118.06(10)	118.60(9)	Fe2−S4−Fe3	73.43(7)	73.73(7)
			Fe3−S4−Fe1	73.82(8)	74.03(7)
S1−Fe1−S5	118.58(11)	119.10(10)	mean of 3	72.72	72.97
S3−Fe2−S6	114.35(10)	114.16(9)			
S2−Fe3−S7	115.23(10)	115.16(9)	Fe1−S5−C4	108.5(3)	108.7(3)
			Fe2−S6−C13	108.4(3)	108.1(3)
M−C1−O1	177.7(9)	178.7(8)	Fe3−S7−C22	104.7(3)	104.0(3)
M−C2−O2	175.8(8)	176.7(8)			
M−C3−O3	175.6(9)	177.8(9)			

The Mössbauer spectrum of **10** in solution (Figure 3) is not resolvably split into overlapping doublets. However, the higher velocity component is broader; the spectrum can be fit with parameters insignificantly different from those of the authentic cuboidal cluster **9** (Table 2). Like **9**, cluster **10** is stable in anaerobic solutions for days at room temperature without detectable decomposition.

Clusters **11** and **12** were generated also by reaction 4 with CO passed directly through the reaction solutions. In the case of **11**, no other cluster signals were observable upon initial formation and for about 2−3 h thereafter. The signals occur in the 8−16 ppm range (Figure 5), and the value $\mu_{eff} = 5.18\ \mu_B$ is close to that of **10**. The 1:10:1 **3**:$NaPF_6$:CO system rapidly lost the signals of **3**, which were replaced by the characteristic methylene signal of $[Fe_4S_4(SEt)_4]^{2-}$ at 12.7 ppm and a 57.9 ppm feature (Figure 5) that cannot be assigned to any known Mo/Fe−S−SEt cluster. Because of its large downfield shift, we assign this signal to cuboidal cluster **12**. An analogous broad signal at 59.3 ppm is generated when, in parallel to reaction 1, $[Fe_4S_4(SEt)_4]^{2-}$ in Me_2SO solution is treated with $Meida^{2-}$ with the intention of forming $[Fe_3S_4(SEt)_3]^{3-}$. The formation of this cluster was always accompanied by a substantial quantity of $[Fe_4S_4(SEt)_4]^{2-}$. In the system shown in Figure 5, the mole ratio $[Fe_4S_4(SEt)_4]^{2-}$:**12** ≈ 20:1. The occurrence of reactions 3 and 4 demonstrates the interconversion of $[Fe_3S_4]^0$ and $[MoFe_3S_4]^0$ clusters.

The formula "$[NaFe_3S_4(SR)_3]^{2-}$" is used to convey the observation that in acetonitrile solutions of the cluster the chemical shifts are dependent on the concentration of $NaPF_6$. This implies the equilibrium $[Fe_3S_4(SR)_3]^{3-} + Na^+ \rightleftarrows [NaFe_3S_4(SR)_3]^{2-}$. While we have not examined the matter in any detail, it is clear that Na^+ stabilizes cuboidal clusters against decomposition to other cluster species, such as has been observed with $[Fe_3S_4(Smes)_3]^{3-}$ [32] in the absence of Na^+. In the presence or absence of Na^+, the ligand dependence of the stability of $[Fe_3S_4(SR)_3]^{3-}$ clusters is clearly $LS_3^{3-} >> mesS^- >>> EtS^-$. It is unlikely that cluster **12** can be isolated as a pure compound.

Electron Transfer Reactions. Potentials for the redox reactions of clusters **3**−**9**, together with coulometric data for selected clusters, are presented in Table 4. Unless noted otherwise, all reactions are electrochemically reversible on the basis of the criteria that E_p and $i_p/\upsilon^{1/2}$ are independent of scan rate (υ) and $i_p/i_a \approx 1$. Two issues arise: (i) correct assignment of redox couple to potential for clusters **3**−**8**; (ii) locus of electron density change pursuant to a redox reaction which, given the core structure, is likely to be centered in either in the Fe_3S_4 portion or the M center.

---

(32) This cluster was generated in acetonitrile solution by a reaction analogous to (1). While its spectrum (*m*-H, 14.35; *p*-Me, 13.50; *o*-Me, 9.9 (br) ppm) appears within 5 min and maximizes in intensity at 20−30 min, it is very weak at 150−170 min. The decomposition process is complicated. Other than the signals of $[Fe_3S_4(Smes)_3]^{3-}$ and $[Fe(Meida)_2]^{2-}$, resonances arising from $[Fe_nS_n(SEt)_4]^{2-}$ (n = 2, 4) and at least two unidentified paramagnetic species are observed over the 170 min interval. After *ca*. 120 min, $[Fe_4S_4(SEt)_4]^{2-}$ is the dominant cluster species. In contrast, note the above observation that **11** can be generated cleanly in solution and gives no NMR-detectable byproducts for at least 2−3 h.

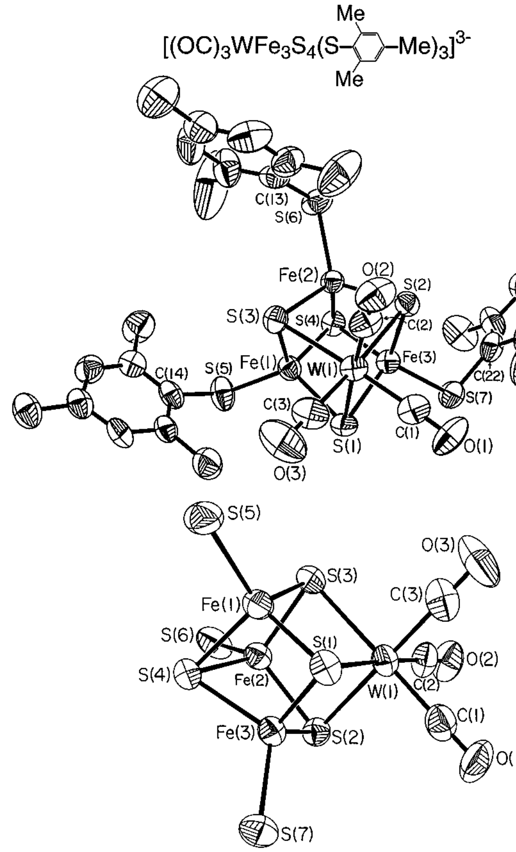

Figure 4. Structure of $[(OC)_3WFe_3S_4(Smes)_3]^{3-}$ as its Et_4N^+ salt, acetonitrile monosolvate, showing 50% probability ellipsoids and the atom labeling scheme. Top: entire cluster. Bottom: cluster without mesityl groups emphasizing idealized trigonal symmetry, with the C_3 axis passing through atoms W1 and S4. $(Et_4N)_3[(OC)_3MoFe_3S_4(Smes)_3]\cdot MeCN$ is isomorphous and isostructural.

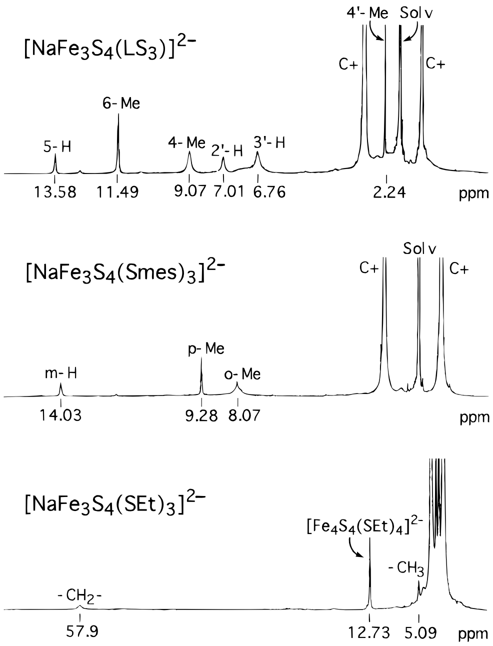

Figure 5. ^{1}H NMR spectra of $[NaFe_3S_4(LS_3)]^{2-}$, $[NaFe_3S_4(Smes)_3]^{2-}$, and $[NaFe_3S_4(SEt)_3]^{2-}$ generated in CD_3CN solutions by the reaction of the appropriate cluster $[(OC)_3MoFe_3S_4(SR)_3]^{3-}$ with CO and $NaPF_6$. Reaction conditions are described in the Experimental Section; signal assignments are indicated.

(1) Redox Series. We have previously shown that cuboidal cluster **9** forms the three-member series (5) encompassing the core oxidation states $[Fe_3S_4]^{+,0,-}$.[8] Thus far, only the $[Fe_3S_4]^0$ state has been isolated. Coulometry of the 2−/3− couple confirmed a one-electron reaction.

$$[Fe_3S_4(LS_3)]^{2-} \overset{e^-}{\rightleftharpoons} [Fe_3S_4(LS_3)]^{3-} \overset{e^-}{\rightleftharpoons} [Fe_3S_4(LS_3)]^{4-} \qquad (5)$$

The 3−/4− couple has the same peak currents, but the apparent instability of the reduced form prevented an accurate coulometric measurement. The cyclic voltammograms of molybdenum/tungsten cluster pairs are presented in the Figures 6 (**5**/**6**) and 7 (**7**/**8**). Clusters **3**−**8** all exhibit the four-member electron transfer series (6). The ligand

$$\begin{array}{ll} \underset{\{M^+/[Fe_3S_4]^+\}}{[(OC)_3MFe_3S_4(SR)_3]^-} \overset{e^-}{\rightleftharpoons} \underset{\{M^0/[Fe_3S_4]^+\}}{[(OC)_3MFe_3S_4(SR)_3]^{2-}} \overset{e^-}{\rightleftharpoons} & \\ \qquad \underset{\{M^0/[Fe_3S_4]^0\}}{[(OC)_3MFe_3S_4(SR)_3]^{3-}} \overset{e^-}{\rightleftharpoons} \underset{\{M^0/[Fe_3S_4]^-\}}{[(OC)_3MFe_3S_4(SR)_3]^{4-}} & (6) \end{array}$$

trend of less negative redox potentials—$LS_3^{3-} > mesS^- \gtrsim EtS^-$—follows that for Fe_4S_4 clusters at parity of charge.[15b,33] For each of the three cluster pairs in each redox step, $E_{Mo} > E_W$, consistent with the fact that tungsten complexes are generally more easily oxidized than their molybdenum analogues. However, the differences are quite small, ranging from 10 to 80 mV; six of the nine values are ≤50 mV. In comparison, clusters containing the more usual cubane-type MFe_3S_4 core in which the M = Mo or W atom is tightly bound (vide supra) show considerably larger differences. For example, in the redox series (7) for triply bridged double cubanes, the potential difference $E_{Mo} - E_W = 110$ mV for both steps.[34] In other cases, $E_{Mo} - E_W$ values over the $[MFe_3S_4]^{4+,3+,2+}$ states of single cubanes[35] and another type of double cubane[36] occur in the range 90−200 mV, with the majority being ≥100 mV. In all cases, the electroactive orbital is mainly Fe−S in character,[37] the members of series 6 being the currently limiting examples in this regard.

$$[M_2Fe_6S_8(SEt)_9]^{3-} \overset{e^-}{\rightleftharpoons} [M_2Fe_6S_8(SEt)_9]^{4-} \overset{e^-}{\rightleftharpoons} [M_2Fe_6S_8(SEt)_9]^{5-} \qquad (7)$$

The potentials of three M = Mo series 6 (Table 4) are not in agreement with a previous assignment of redox couples to potentials.[16b] For **3** in dichloromethane, the 2−/3− couple was assigned to −0.36 V and the 3−/4− couple to −0.89 V. These electron transfer reactions were attributed to the core series (8), in which the neutral core was

$$[MoFe_3S_4]^+ \overset{e^-}{\rightleftharpoons} [MoFe_3S_4]^0 \overset{e^-}{\rightleftharpoons} [MoFe_3S_4]^- \qquad (8)$$

shown by Mössbauer spectroscopy to contain the $[Fe_3S_4]^0$ fragment, thus fixing the heterometal as Mo(0). The most reduced core would then be formulated as $[Fe_3S_4]^- +$ Mo(0). Charge distribution within the unipositive core was not specified. Potentials of variously ligated clusters $[(OC)_3MoFe_3S_4L_3]^{3-}$ were assigned analogously.[16b] The core oxidation states of series 8 are found in series 6, which also encompasses the previously undetected state $[MoFe_3S_4]^{2+}$. In terms of overall charge, the previous assignment places the 2−/3− couple at *ca.* −0.3 V whereas our results require it to be nearer −0.8 V. Likewise, the 3−/4− couple at *ca.* −0.9 V does not agree with the present data which locate it in the vicinity of −1.4 to −1.7 V. If **7** and **9** with the same ligand are compared under the previous assignment, the $[Fe_3S_4]^+$ and $[Fe_3S_4]^0$ states of the former are stabilized to reduction by 460 and 550 mV, respectively. These and related differences in potential (Table 4) appeared to be implausibly large and have occasioned a more extensive study of the redox reactions of $[(OC)_3MFe_3S_4(SR)_3]^{3-}$ clusters.

In examining electron transfer series 6, we have made use of electrochemical methods to address issue i and FTIR spectroscopy for

---

(33) Weigel, J. A.; Holm, R. H. *J. Am. Chem. Soc.* **1991**, *113*, 4184.

(34) Wolff, T. E.; Power, P. P.; Frankel, R. B.; Holm, R. H. *J. Am. Chem. Soc.* **1980**, *102*, 4694.

(35) (a) Armstrong, W. H.; Mascharak, P. K.; Holm, R. H. *J. Am. Chem. Soc.* **1982**, *104*, 4373. (b) Mascharak, P. K.; Armstrong, W. H.; Mizobe, Y.; Holm, R. H. *J. Am. Chem. Soc.* **1983**, *105*, 475.

(36) Huang, J.; Goh, G.; Holm, R. H. *Inorg. Chem.* **1997**, *36*, 356.

(37) This point has been demonstrated by Mössbauer spectroscopic studies of the series $[Mo_2Fe_6S_8(SPh)_9]^{3-,4-,5-}$: Christou, G.; Mascharak, P. K.; Amstrong, W. H.; Papefthymiou, G. C.; Frankel, R. B.; Holm, R. H. *J. Am. Chem. Soc.* **1982**, *104*, 2820.

Table 4. Electrochemical Data for $[(OC)_3MFe_3S_4(SR)_3]^{3-}$ and $M(CO)_3(ttcn)$ (M = Mo, W) in Acetonitrile

cluster	$E_{1/2}$,[a] V 1+/0	1−/2−	2−/3−	3−/4−	$n(e^-)$ 1−/2−/3−
$[Fe_3S_4(LS_3)]^{3-}$ (**9**)			−0.79	−1.72	0.8[b]
$[(OC)_3MoFe_3S_4(SEt)_3]^{3-}$ (**3**)		−0.32	−0.88	−1.67	*c*
$[(OC)_3WFe_3S_4(SEt)_3]^{3-}$ (**4**)		−0.34	−0.95	−1.62	*c*
$[(OC)_3MoFe_3S_4(Smes)_3]^{3-}$ (**5**)		−0.31	−0.86	−1.54	2.0[d]
$[(OC)_3WFe_3S_4(Smes)_3]^{3-}$ (**6**)		−0.34	−0.94	−1.55	1.9[d]
$[(OC)_3MoFe_3S_4(LS)_3]^{3-}$ (**7**)		−0.23	−0.78	−1.43	2.1[d]
$[(OC)_3WFe_3S_4(LS_3)]^{3-}$ (**8**)		−0.25	−0.84	−1.41	2.3[d]
$Mo(CO)_3(ttcn)$ (**13**)	+0.52				*e*
$W(CO)_3(ttcn)$ (**14**)	+0.48				*e*

[a] 298 K; vs SCE. $E_{1/2} = (E_{pc} + E_{pa})/2$. [b] 2−/3− couple; potential set at −0.62 V vs SCE. [c] Not determined. [d] Potential set at 0.00 V vs SCE. [e] Poorly behaved in coulometry.

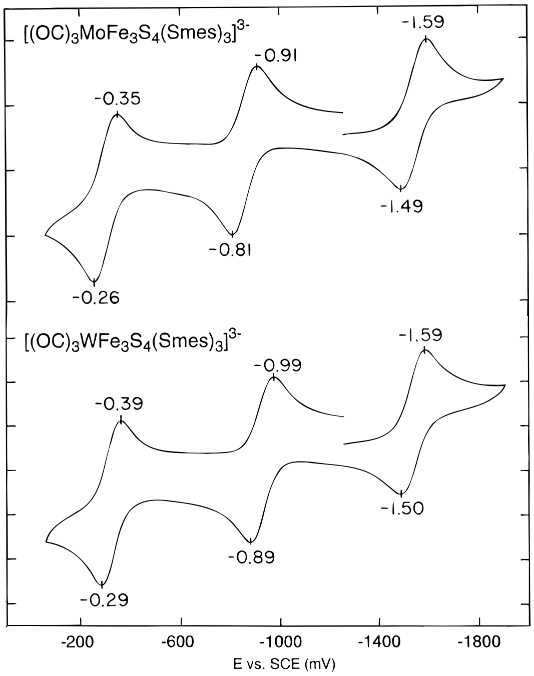

Figure 6. Cyclic voltammograms (100 mV/s) of $[(OC)_3MFe_3S_4(Smes)_3]^{3-}$ (M = Mo, W) in acetonitrile solutions. Peak potentials are indicated.

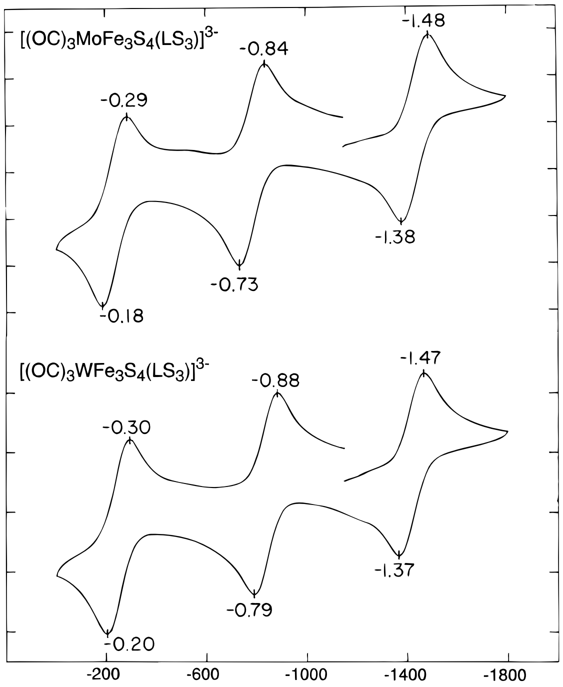

Figure 7. Cyclic voltammograms (100 mV/s) of $[(OC)_3MFe_3S_4(LS_3)]^{3-}$ (M = Mo, W) in acetonitrile solutions. Peak potentials are indicated.

Table 5. Infrared Spectral Data for $[(OC)_3MFe_3S_4(SR)_3]^{3-}$ and $M(CO)_3(ttcn)$ (M = Mo, W) in Various Oxidation States Determined in OTTLE Cell Experiments in Acetonitrile

cluster	ν_{CO}, cm^{-1} 1+	0	1−	2−	3−	4−
$[(OC)_3MoFe_3S_4(Smes)_3]^{3-}$ (**5**)			*a*	1966 1887	1872 1766	1854[b] 1726[b]
$[(OC)_3WFe_3S_4(Smes)_3]^{3-}$ (**6**)			2044 1995	1959 1879	1861 1763	1842[b] 1701[b]
$[(OC)_3MoFe_3S_4(LS_3)]^{3-}$ (**7**)			*a*	1972 1911	1875 1768	1858 1726
$[(OC)_3WFe_3S_4(LS_3)]^{3-}$ (**8**)			2054 1996	1964 1898	1864 1767	1845 1715
$Mo(CO)_3(ttcn)$ (**13**)	2069 2002	1932 1822				
$W(CO)_3(ttcn)$ (**14**)	2060 1983	1925 1816				

[a] Poorly defined feature. [b] Shoulder.

issue ii. The use of an OTTLE cell allows for the determination of carbonyl stretching frequencies of clusters in different oxidation states. Under our experimental conditions, the region 1600−2100 cm^{-1} was free of significant solvent or electrolyte absorption. This region was monitored at set potentials as a function of time, with an electrolysis typically completed in less than 4 min. The body of stretching frequencies measured in this way is assembled in Table 5. For clusters **5**−**8**, all oxidation states could be nearly reversibly generated, with about a 10% loss in band intensity through each cycle. The two-electron-oxidized forms of molybdenum clusters **5** and **7** were not observed, presumably due to instability. Clusters **3** and **4** did not exhibit clean redox conversions in the OTTLE cell; generation of $[M(CO)_{6-n}(MeCN)_n]$ and free CO was observed. All four oxidation states of tungsten clusters **6** and **8** were achieved. We discuss the IR behavior of cluster **8** in some detail; where the data are available, they show that **5**−**7** behave in a strictly analogous manner.

(2) The 2−/3−/4− Steps of Series 6. In coulometric experiments with clusters **5**−**8** in acetonitrile, the potential was set at 0.00 V and the current monitored. Each cluster was oxidized by two electrons, indicating that the first two processes, at the less negative potentials, are oxidations, a result supported by the resting potentials of the systems, which were *ca.* −1.15 V. These results lead to the correlation of redox couples and potentials in Table 4.

The 3−/4− couple is the terminal event in series 6. Potential differences between molybdenum and tungsten cluster pairs are practically nil. However, the $M(CO)_3$ groups are not without an effect on potentials. Without exception, the potentials are less negative than that of the 3−/4− couple of **9**, the differences ranging from 50 mV (**3**) to 310 mV (**8**). The $M(CO)_3$ group is, effectively, an electron-withdrawing substituent, rendering the $[Fe_3S_4]^0$ fragment more easily reduced than in its absence. IR spectra for the 3−/4− couple of **8** are shown in Figure 8. The 3− cluster exhibits bands at 1864 and 1767 cm^{-1}. As the electrolysis proceeds, these bands become less intense and those of the 4− cluster grow in at 1845 and 1715 cm^{-1}. Reduction

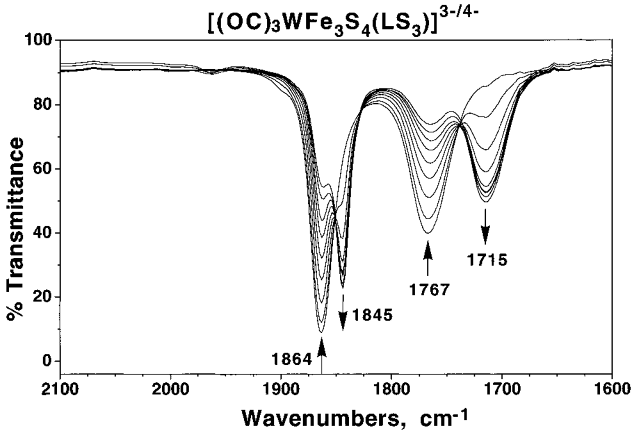

Figure 8. Infrared spectra collected during the reduction of $[(OC)_3WFe_3S_4(LS_3)]^{3-}$ in an OTTLE cell at regular time intervals (30 s, acetonitrile solution, 0.1 M $(Bu_4N)(PF_6)$). Arrows indicate the appearance and disappearance of bands (cm^{-1}) during the course of the experiment.

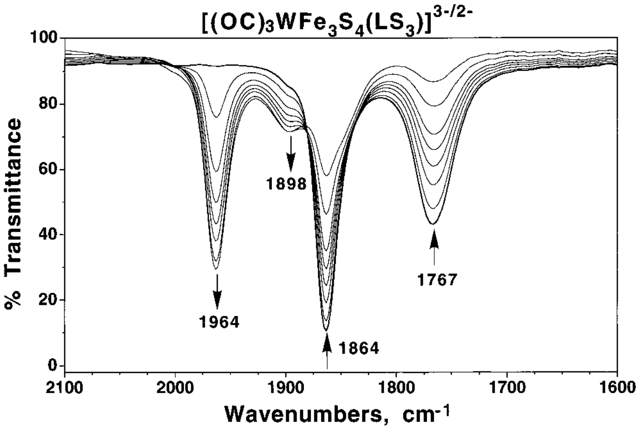

Figure 9. Infrared spectra collected during the oxidation of $[(OC)_3WFe_3S_4(LS_3)]^{3-}$ in an OTTLE cell under the conditions of Figure 8.

increases the electron density of the cluster and appreciably influences ν_{CO} values, causing them to decrease as the extent of M−CO back-bonding increases. For the reduction of **5**−**7**, typical decreases are about 25 cm^{-1} for the asymmetric stretch and 50 cm^{-1} for the symmetric stretch. Even though the reduction process is, sensibly, $[Fe_3S_4]^{0/-}$ and some (slight) fraction of added electron density is presumably distributed on the LS_3 ligand, enough remains to be delocalized in the $M(CO)_3$ group. The low-frequency ν_{CO} shifts are one manifestation of the electron-withdrawing nature of these groups detected electrochemically.

IR spectra for the 3−/2− oxidation of **8** are provided in Figure 9. There is a large increase in both ν_{CO} features, from 1864 to 1964 cm^{-1} for the asymmetric stretch and from 1767 to 1898 cm^{-1} for the symmetric stretch. Comparable ν_{CO} shifts in are observed for **5**−**7**. In these cases, diminution of core electron density has the expected effect of raising frequencies. The 3−/2− step in series 6 is concluded to result in the core change $[Fe_3S_4]^{0/+}$ rather than $Mo^{0/+}$, a process which appears unlikely to occur around −0.8 V at a molybdenum center with tricarbonyl ligation. Again, however, these components are clearly electronically coupled, given the appreciable increases in ν_{CO} upon oxidation (100 and 121 cm^{-1} for **8**).

(3) The 2−/1− Step of Series 6. The $Mo^0/[Fe_3S_4]^+$ formulation of dinegative clusters implicates the most oxidized state known for cuboidal Fe_3S_4 (series 5). The 2−/1− step is unlikely to involve oxidation of the all-ferric core to one with Fe(IV) character, a property unprecedented in clusters with terminal thiolate ligation and one that is likely to lead to an autoredox event. It is more reasonable to assign this process to oxidation of the heterometal. To investigate the possibility of a heterometal-centered redox process, the electrochemistry of mononuclear complexes **13** and **14** has been examined. The two complexes are isostructural;[21,22] the ttcn sulfur atoms roughly simulate the bonding function of the μ_3-S atoms bound to the heterometal in **3**−**8**. The cyclic voltammograms in Figure 10 reveal reversible one-electron oxidations at +0.52 V (**13**) and +0.48 V (**14**). While these potentials are considerably more positive that those of the clusters, they support the proposition that $M^0(CO)_3S_3$ coordination units can be oxidized. The positive shifts are mainly a consequence of zero net charge of the molecules. When **13** and **14** are oxidized to $[M(CO)_3(ttcn)]^+$, ν_{CO} values sharply increase: 137 and 180 cm^{-1} for M = Mo and 135 and 167 cm^{-1} for M = W. Further oxidation of **8** to the 1− species[38] generates new bands at 2054 and 1996 cm^{-1}, increased by 90 and 98 cm^{-1}, respectively, over the 2− cluster and about 200 cm^{-1} above the ν_{CO} values of **8** in the 3− state. Comparable changes are observed for **6** (Table 5). These frequency increases are not as large of those for **13** and **14**, which are intended as rough calibrants for metal-centered oxidations. The difference in the increases likely arises from the more polarizable sulfide donor atoms in the clusters, which are more effective than thioether sulfur atoms in compensating for a decrease in electron density at the M site. We conclude that the 1− clusters are best described as $M^+/[Fe_3S_4]^+$.

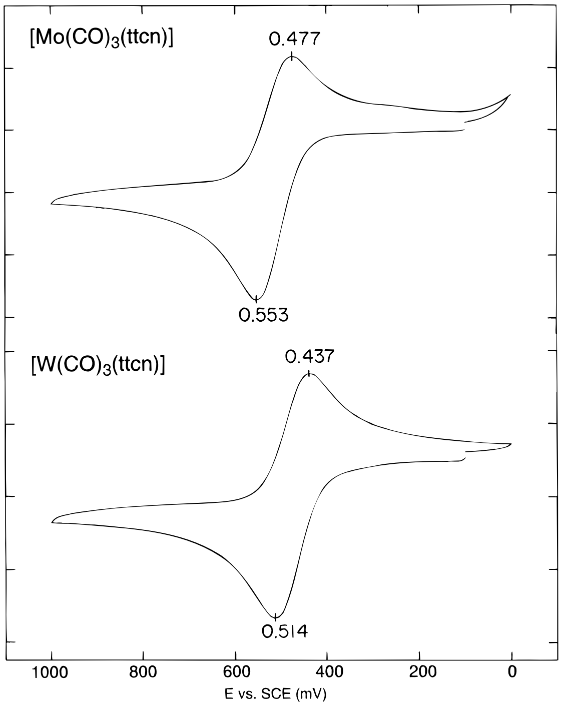

Figure 10. Cyclic voltammograms (100 mV/s) of $[M(CO)_3(ttcn)]$ (M = Mo, W) in acetonitrile solutions. Peak potentials are indicated.

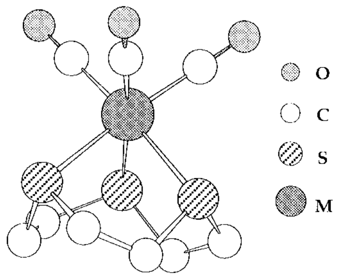

13/14

Summary

The following are the principal results and conclusions of this investigation.

---

[38] Both this species and $[M(CO)_3(ttcn)]^+$ have limited stability under OTTLE cell conditions. However, their carbonyl bands are adequately intense and were identified by intensity changes during the period of electrolysis.

(1) The clusters $[(OC)_3MFe_3S_4(Smes)_3]^{3-}$ (M = Mo, W) exhibit conspicuously long M−S (2.62, 2.59 Å) and M−Fe (3.22, 3.19 Å) distances which, together with earlier results for $[(OC)_3MoFe_3S_4(SEt)_3]^{3-}$, ensure that these are inherent properties of $[MFe_3S_4]^0$ clusters with terminal tricarbonyl ligation at the M site. These weak interactions potentiate the removal of the $M(CO)_3$ group.

(2) Clusters with cores $[Fe_3S_4]^0$ and $[MFe_3S_4]^0$ (M = Mo, W) can be interconverted by reaction of the former with $[M(CO)_3(MeCN)_3]$ (reaction 3) and reaction of the latter with CO in the presence of sodium ion. Reaction **4** is a second synthetic route to $[Fe_3S_4]^0$ clusters, which serve as synthetic analogues[8] of $[Fe_3S_4(S{\cdot}Cys)_3]^{3-}$ centers in proteins.

(3) The order of the ligand dependence of the stability of the $[Fe_3S_4(SR)_3]^{3-}$ clusters is LS_3^{3-} followed by 2,4,6-trimethylbenzenethiolate and then ethanethiolate, in the presence or absence of sodium ion. The cluster $[Fe_3S_4(LS_3)]^{3-}$ is by far the most stable of the three.

(4) The clusters $[(OC)_3MFe_3S_4(SR)_3]^{3-}$ form a *four*-membered electron transfer series whose members are related by reversible one-electron reactions. The trianionic clusters can be once reduced and twice oxidized to afford series 6.

(5) The correct assignments of redox couple to potential in series 6 are those in Table 4 for three series each of molybdenum and tungsten clusters. Under these assignments, the $M(CO)_3$ group perturbs the potentials of the parent $[Fe_3S_4]^0$ cluster in the form of positive shifts, demonstrating that the group is electron-withdrawing.

(6) Carbonyl stretching frequencies are notably sensitive to changes in cluster oxidation state, shifting to lower values upon reduction and higher values upon oxidation. The low-energy shifts are consistent with the displacement of potentials in point 5. Appreciable shifts are observed even in those cases where the redox reaction is not M-centered. Consequently, the $M(CO)_3$ and Fe_3S_4 portions of $[MFe_3S_4]^{2+,+,0,-}$ clusters are demonstrably electronically coupled despite the long bond lengths in point 1. Limiting oxidation state descriptions are included in series 6.

With the direct insertion of heterometal groups into cuboidal $[Fe_3S_4(LS_3)]^{3-}$ demonstrated, and the effects of those groups on the potentials of $[(OC)_3MFe_3S_4(SR)_3]^{3-}$ product clusters determined, we have commenced an investigation addressing the scope of heterometal incorporation reactions and the effects of heterometals on the properties of the resultant $[MFe_3S_4]^z$ clusters.[17]

Acknowledgment. This research was supported by NIH Grant GM 28856. X-ray diffraction equipment was obtained by NIH Grant 1 S10 RR 02247. C.A.C. thanks the National Institutes of Health for a postdoctoral fellowship.

Supporting Information Available: Tables of crystal and intensity collection data, atom positional and thermal parameters, and bond angles and distances (28 pages). Ordering information is given on any current masthead page.

IC961122O